

Subject: SOI – Geophysical Field Assistance

Date: 23 May 2003

To: Patricia S. Leavenworth
State Conservationist
6515 Watts Road, Suite 200
Madison, Wisconsin 53719-2726

Purpose:

To assess the suitability of ground-penetrating radar (GPR) for soil and bedrock investigations in Iron County. In addition, training was provided on the use and operation of both GPR and electromagnetic induction (EMI) to participating soil scientists.

Participants:

Jim Barnes, Price County Project Leader, USDA-NRCS, Phillips, WI
Jim Doolittle, Research Soil Scientist, USDA-NRCS-NSSC, Newtown Square, PA
Mark Farina, Soil Scientist, USDA-NRCS, Ironwood, WI
David Hvizdak, Resource Soil Scientist, USDA-NRCS, Spooner, WI
Terry Kroll, Soil Scientist, USDA-NRCS, Ashland, WI
Mark Krupiuski, Bayfield Subset Project Leader, USDA-NRCS, Spooner, WI
John Lucassen, MLRA Project Leader, USDA-NRCS, Ashland, WI
Fred Madison, Professor of Soils, University of Wisconsin, Madison, WI
Jennifer Maziasz, Soil Scientist, USDA-NRCS, Ashland, WI
Bill Perkis, Gogebic County Project Leader, USDA-NRCS, Ironwood, WI
Darin Silkworth, Soil Scientist, USDA-NRCS, Ironwood, WI
Fred Simeth, MLRA Project Leader, USDA-NRCS, Spooner, WI
Jeff Talsky, Soil Scientist, USDA-NRCS, Spooner, WI
Kevin Traastad, Soil Scientist, USDA-NRCS, Phillips, WI
Jesse Turk, Soil Scientist, USDA-NRCS, Ashland, WI

Activities:

All activities were completed during the period of 19 to 23 May 2003.

Summary:

1. In many upland areas of northern Wisconsin is exceedingly difficult and impractical to determine bedrock depths with traditional soil survey tools. Numerous rock fragments severely limit the effectiveness of shovels and augers. Soil scientists spend unwarranted amount of time and energy attempting to determine the depth to bedrock only to be refused, in many instances, by rock fragments. In addition, doubts arise as to whether auger penetration was restricted by a large rock fragment or bedrock.
2. Ground-penetrating radar was found to be more efficient and effective than traditional soil survey tools for bedrock determinations. The use of GPR will greatly facilitate the documentation of bedrock depths and improve map unit design based on soil-depth criteria. Based on the positive response of all participants, further use of GPR is encouraged.
3. Training was provided to soil scientist on the use and operation of GPR and EMI. Many participants had the opportunity to operate, complete field surveys, and evaluate the use of the EM38DD meter for soil survey investigations.

4. Electromagnetic induction was used to create detailed maps showing the spatial distribution of apparent conductivity across units of management. These maps closely corresponded with the distribution of soils and soil properties shown on soil maps. In each delineation, trends and included areas were shown with EMI maps.
5. To assist EMI interpretations, computer simulations are normally used. ArcView GIS has become available to many soil scientists and field offices. Integration of EMI and ArcView GIS techniques provides a more expedient and cost-effective method for displaying EMI data, soil mapping, and multiple data sets.

It was my pleasure to work once again in Wisconsin and with members of your fine staff.

With kind regards,

James A. Doolittle
Research Soil Scientist
National Soil Survey Center

cc:

- R. Ahrens, Director, USDA-USDA, National Soil Survey Center, Federal Building, Room 152, 100 Centennial Mall North, Lincoln, NE 68508-3866
- J. W. Hempel, State Soil Scientist, , USDA-NRCS, 6515 Watts Road, Suite 200, Madison, Wisconsin 53719-2726
- J. A. Lucassen, MLRA Project Leader, USDA-NRCS, 315 Sanborn Avenue, Suite 100, P.O. Box 267, Ashland, WI 54806-1032
- W. Maresch, Acting Director of Soils Survey Division, USDA-NRCS, Room 4250 South Building, 14th & Independence Ave. SW, Washington, DC 20250
- J. McCloskey, Region 10 M.O. Team Leader, USDA-NRCS, 375 Jackson Street, Suite 600, St. Paul, MN 55101-1854
- C. Olson, National Leader for Soil Investigations, USDA-USDA, National Soil Survey Center, Federal Building, Room 152, 100 Centennial Mall North, Lincoln, NE 68508-3866
- W. Tuttle, Soil Scientist (Geophysical), USDA-NRCS-NSSC, P.O. Box 974, Federal Building, Room 206, 207 West Main Street, Wilkesboro, NC 28697

Equipment:

The radar unit is the Subsurface Interface Radar (SIR) System-2000, manufactured by Geophysical Survey Systems, Inc.¹ Morey (1974), Doolittle (1987), and Daniels (1996) have discussed the use and operation of GPR. The SIR System-2000 consists of a digital control unit (DC-2000) with keypad, VGA video screen, and connector panel. A 12-volt battery powers the system. This unit is backpack portable and, with an antenna, requires two people to operate. A 400 MHz antenna was used in this investigation.

The EM38DD meter, manufactured by Geonics limited, was used in this study.¹ This meter is portable and need only one person to operate. No ground contact is required with this meter. This device measured the apparent conductivity of the underlying earthen materials. Values of apparent conductivity are expressed in milliSiemens per meter (mS/m). Lateral resolution is approximately equal to the intercoil spacing. Geonics Limited (2000) describes the operating procedures of EM38DD meter. The EM38DD meter has a 1-m intercoil spacing and operates at a frequency of 14,600 Hz. It has effective penetration depths of about 0.75 and 1.5 m in the horizontal and vertical dipole orientations, respectively (Geonics Limited, 2000). The EM38DD meter consists of two EM38 meters bolted together and electronically coupled. One meter acts as a master unit (meter that is positioned in the vertical dipole orientation and having both transmitter and receiver activated) and one meter acts as a slave unit (meter that is positioned in the horizontal dipole orientation with only the receiver switched on).

The Geonics DAS70 Data Acquisition System was used to record and store EMI data.¹ The acquisition system consists of either an EM31 or EM38DDmeter and Allegro field computer. With this data acquisition system, the meter is keypad operated and measurements can either be automatically or manually triggered.

To help summarize the results of this study, the SURFER for Windows (version 8) program, developed by Golden Software, Inc.,¹ was used to construct two-dimensional simulations. Grids were created using kriging methods with an octant search.

GPR:**Background:**

In many upland areas of northern Wisconsin is exceedingly difficult and impractical to determine bedrock depths with traditional soil survey tools. Numerous rock fragments restrict observation depths of shovels and augers. Soil scientists spend inordinate amount of time and energy attempting to determine the depth to bedrock only to be refused, in many instances, by rock fragments. In addition, uncertainties arise as to whether auger penetration was restricted by a large rock fragment or bedrock. While backhoes provide accurate and reliable soil depth information, however, backhoes can only provide limited or partial information. Typically, backhoe pits are limited in number and widely spaced. Inferences on the depth to bedrock must be extended across the more expansive areas between a limited number of pits. As a consequence, the composition of soil map units based on soil-depth criteria is constrained by limited exposures and burdened by partial, detached, or inadequate data.

In many areas, ground-penetrating radar is well suited to soil-bedrock determinations. Collins and others (1989) demonstrated that GPR was more reliable and effective than soil auger used by soil scientist to map bedrock depths. These researchers found a high ($r = 0.98$) and significant (0.01 level) between excavated and radar interpreted depths to bedrock. In this study, the average difference between actual and radar interpreted depths to bedrock was only 6 cm with 87% of the observations within 10 cm. For depths to bedrock less than 4 m, Birkhead and others (1996) observed an average error between observed and radar interpreted measurements of 4.4 %.

Field Procedures:

Pulling the 400 MHz antenna by hand across soil map units completed radar surveys. Soil delineations were selected to cover a large geographic area in iron and Bayfield counties. Although, GPR provides a continuous profile of subsurface conditions, interpretations were restricted to observation points. For each transect, observation points were spaced at distances of either 10 or 15 paces. At each observation point, the radar operator

¹ Trade names are used to provide specific information. Their mention does not constitute endorsement by USDA-NRCS.

impressed a dashed, vertical line on the radar profile. This line identified the observation point on the radar record. A total of observation points were recorded during this field assignment.

Each radar traverse was stored as a separate file on a hard disc. For each radar record, depth to bedrock was interpreted directly on the SIR-2000's VGA video screen. All interpretations were made from color-enhanced images visible on this computer screen. Different color transforms were used to interpret the depths to bedrock. Numerous chaotic reflectors from rock fragments of various sizes and shapes characterized the till. The lithic contact generally appeared as a high amplitude reflector. The underlying bedrock often lacked reflectors. This interface was highly irregular on most radar records. Laterally, this interface was interspersed with both high and low amplitude reflectors. At each observation point, the depth to bedrock was interpreted on the radar record.

Study Sites:

Sites for GPR bedrock determinations were located in different parts of Iron County. All sites were located in wooded areas. Table 1 lists the radar record numbers and the names and locations of the traversed soil map units. Thirty-one radar traverses were conducted in nine different soil map units. The depth to bedrock was interpreted at 349 observation points.

Table 1. Locations of map units surveyed with GPR

File	Soil	Location
1	Michigamme-Channing sil, 0-3 % slope, extremely stoney	SE1/4 SEC 1 T 46 N R 1 E
3	Michigamme sil, 3-6% slope, extremely stoney	SW1/4 SEC 1 T 46 N R 1 E
4	Michigamme sil, 6-9% slope, extremely stoney	SW1/4 SEC 1 T 46 N R 1 E
5	Michigamme sil, 3-6% slope, extremely stoney	SW1/4 SEC 1 T 46 N R 1 E
6	Michigamme sil, 3-6% slope, extremely stoney	SW1/4 SEC 1 T 46 N R 1 E
7	Michigamme sil, 3-6% slope, extremely stoney	SW1/4 SEC 1 T 46 N R 1 E
8	Michigamme sil, 3-6% slope, extremely stoney	SW1/4 SEC 1 T 46 N R 1 E
9	Michigamme sil, 3-6% slope, extremely stoney	SW1/4 SEC 1 T 46 N R 1 E
10	Dishno-Tula-Rock Outcrop complex, 0-18% slope, extremely stoney	SW1/4 SEC 10 T 46 N R 1 E
11	Dishno-Tula-Rock Outcrop complex, 0-18% slope, extremely stoney	SW1/4 SEC 10 T 46 N R 1 E
12	Tula-Dishno-Rock Outcrop sil 0-6% slopes, stoney	SW1/4 SEC 10 T 46 N R 1 E
13	Tula-Dishno-Rock Outcrop sil 0-6% slopes, stoney	SW1/4 SEC 10 T 46 N R 1 E
14	Tula-Dishno-Rock Outcrop sil 0-6% slopes, stoney	SW1/4 SEC 10 T 46 N R 1 E
17	Dishno-Gogebic Rock Outcrop, 18-35% slopes, very stoney	SE1/4 SEC 24 T 46 N R 1 E
18	Gogebic bedrock subsurface	NE1/4 SEC 36 T 46 N R 1 E
19	Gogebic bedrock subsurface	NE1/4 SEC 36 T 46 N R 1 E
20	Gogebic bedrock subsurface	NW1/4 SEC 30 T 46 N R 2 E
21	Gogebic bedrock subsurface	NW1/4 SEC 30 T 46 N R 2 E
22	Gogebic bedrock subsurface	NW1/4 SEC 30 T 46 N R 2 E
23	Gogebic bedrock subsurface	NW1/4 SEC 30 T 46 N R 2 E
24	Gogebic sil, 6 to 18% slopes, very stoney, rocky	SW1/4 SEC 34 T 46 N R 1 W
25	Gogebic sil, 6 to 18% slopes, very stoney, rocky	SW1/4 SEC 34 T 46 N R 1 W
26	Gogebic sil, 6 to 18% slopes, very stoney, rocky	SW1/4 SEC 34 T 46 N R 1 W
27	Gogebic sil, 6 to 18% slopes, very stoney, rocky	SW1/4 SEC 34 T 46 N R 1 W
28	Gogebic sil, 6 to 18% slopes, very stoney, rocky	SW1/4 SEC 34 T 46 N R 1 W
36	Gogebic-Metonga fsl 2 to 10% Slopes	SW1/4 SEC 13 T 45 N R 4 W
37	Gogebic-Metonga fsl 2 to 10% Slopes	SW1/4 SEC 13 T 45 N R 4 W
38	Gogebic-Metonga fsl 2 to 10% Slopes	SW1/4 SEC 13 T 45 N R 4 W
39	Gogebic-Metonga fsl 2 to 10% Slopes	SE1/4 SEC 14 T 45 N R 4 W
40	Gogebic-Metonga fsl 2 to 10% Slopes	SE1/4 SEC 14 T 45 N R 4 W
41	Gogebic-Metonga fsl 2 to 10% Slopes	SE1/4 SEC 14 T 45 N R 4 W

Surveys were conducted in areas of Channing, Dishno, Gogebic, Metonga, Michigamme, and Tula soils on moraines. These soils have high rock fragment contents, which ranged in size from gravels to boulders. The very deep, somewhat poorly drained Channing soil formed in loamy deposits and in the underlying sand and gravel. The deep, moderately well drained Dishno soil formed in a silty or loamy eolian deposits over sandy and gravelly till underlain basalt. The very deep, moderately well drained Gogebic soil formed in modified loamy eolian deposits and in the underlying loamy and sandy glacial till. Gogebic soil is shallow or moderately deep to a fragipan. The moderately deep, well drained and moderately well drained Michigamme soil formed in a silty or loamy mantle over loamy glacial till underlain basalt. The moderately deep, well drained Metonga soil formed in a silty or loamy eolian mantle, or in the eolian mantle and in loamy till underlain by igneous or metamorphic bedrock. The very deep, somewhat poorly drained Tula soil formed in modified loamy eolian material and in the underlying loamy till. Tula soil is shallow to moderately deep to a fragipan.

Table 2. Classification of soils surveyed in GPR bedrock investigations.

Soil Series	Taxonomic Family
Channing	coarse-loamy over sandy or sandy-skeletal, mixed, superactive, frigid Typic Endoaquods
Dishno	coarse-loamy over sandy or sandy-skeletal, mixed, superactive, frigid Oxyaquic Haplorthods
Gogebic	coarse-loamy, mixed, superactive, frigid Alfic Oxyaquic Fragiorthods
Metonga	coarse-loamy, mixed, superactive, frigid Entic Haplorthods
Michigamme	coarse-loamy, mixed, superactive, frigid Typic Haplorthods
Tula	coarse-loamy, mixed, superactive, frigid Argic Fragiaquods

Calibration of GPR:

Ground-penetrating radar is a time scaled system. This system measures the time that it takes electromagnetic energy to travel from the antenna to an interface (e.g., bedrock, soil horizon, stratigraphic layer) and back. To convert the travel time into a depth scale, either the velocity of pulse propagation or the depth to a reflector must be known. The relationships among depth (D), two-way pulse travel time (T), and velocity of propagation (V) are described in the following equation (Morey, 1974):

$$V = 2D/T \quad [1]$$

The velocity of propagation is principally affected by the dielectric permittivity (E) of the profiled material(s) according to the equation:

$$E = (C/V)^2 \quad [2]$$

Where C is the velocity of propagation in a vacuum (about 0.3 m/nanosecond). Velocity is expressed in meters per nanosecond (ns). A nanosecond is one billionth of a second. The amount and physical state of water (temperature dependent) have the greatest effect on the dielectric permittivity of a material.

The velocity of propagation and the depth scale were determined by comparing the interpreted depth to bedrock on the radar record with the depths measured in soil pits. Based on the measured depth and the two-way travel time to this interface, and equation [1], the velocity of propagation was estimated to be about 0.086 m/ns. The dielectric permittivity was 12.

On radar profiles, reflections from interfaces spaced closer than one half wavelength apart are indistinguishable due to constructive and destructive interference (Daniels, 1996). Daniels (1996) used the following equation to show the relationship between velocity of propagation (v), antenna center frequency (f), and wavelength (λ):

$$\lambda = v/f \quad [3]$$

Equation [3] shows that the propagated wavelength will decrease with decreasing propagation velocity and increasing antenna frequency. Using equation [2] and an average velocity of 0.086 m/ns resulted in wavelengths of

about 21 cm (about 8 inches) at a frequency of 400 MHz. Interfaces spaced closer than 8 inches were difficult to identify on radar profiles.

Results:

The results of this investigation are summarized in Table 3 and Appendix 1. Table 3 summarizes interpreted depths to bedrock by soil depth classes. For each transect, the number as well as the frequency of observations for each soil depth class are given. Depth classes are shallow (0 to 20 inches), moderately deep (20 to 40 inches), deep (40 to 60 inches) and very deep (>60 inches). Where bedrock was exposed at the surface, the observation depth was 0 and the depth class was “*outcrop.*” Appendix 1 summarizes the interpreted depths to the bedrock surface for each transect. Depths are expressed in inches.

**Table 3. Summary of Transect Data.
Frequency Distribution of Depths to Bedrock by Soil Depth Classes.**

File	Soil	Obs.	Outcrop	Shallow	Mod. Deep	Deep	Very Deep
1	Michigamme-Channing sil, 0-3 % slope, extremely stoney	10	0.00	0.00	0.40	0.60	0.00
3	Michigamme sil, 3-6% slope, extremely stoney	10	0.00	0.25	0.50	0.25	0.00
4	Michigamme sil, 6-9% slope, extremely stoney	8	0.00	0.13	0.38	0.49	0.00
5	Michigamme sil, 3-6% slope, extremely stoney	14	0.00	0.00	0.57	0.43	0.00
6	Michigamme sil, 3-6% slope, extremely stoney	12	0.00	0.00	0.50	0.50	0.00
7	Michigamme sil, 3-6% slope, extremely stoney	11	0.00	0.09	0.37	0.45	0.09
8	Michigamme sil, 3-6% slope, extremely stoney	11	0.00	0.00	0.91	0.09	0.00
9	Michigamme sil, 3-6% slope, extremely stoney	11	0.00	0.00	0.91	0.09	0.00
10	Dishno-Tula-Rock Outcrop complex, 0-18% slope, extremely stoney	15	0.13	0.27	0.60	0.00	0.00
11	Dishno-Tula-Rock Outcrop complex, 0-18% slope, extremely stoney	12	0.08	0.00	0.75	0.17	0.00
12	Tula-Dishno-Rock Outcrop sil 0-6% slopes, stoney	9	0.00	0.00	0.00	0.11	0.89
13	Tula-Dishno-Rock Outcrop sil 0-6% slopes, stoney	14	0.00	0.00	0.21	0.50	0.29
14	Tula-Dishno-Rock Outcrop sil 0-6% slopes, stoney	13	0.00	0.00	0.40	0.60	0.00
17	Dishno-Gogebic Rock Outcrop, 18-35% slopes, very stoney	13	0.00	0.54	0.23	0.15	0.08
18	Gogebic bedrock subsurface	5	0.00	0.00	0.20	0.60	0.20
19	Gogebic bedrock subsurface	8	0.00	0.25	0.63	0.12	0.00
20	Gogebic bedrock subsurface	10	0.00	0.50	0.50	0.00	0.00
21	Gogebic bedrock subsurface	11	0.00	0.55	0.27	0.18	0.00
22	Gogebic bedrock subsurface	10	0.00	0.60	0.30	0.10	0.00
23	Gogebic bedrock subsurface	3	0.33	0.00	0.00	0.67	0.00
24	Gogebic sil, 6 to 18% slopes, very stoney, rocky	12	0.00	0.00	0.33	0.50	0.17
25	Gogebic sil, 6 to 18% slopes, very stoney, rocky	11	0.00	0.00	0.38	0.62	0.00
26	Gogebic sil, 6 to 18% slopes, very stoney, rocky	13	0.00	0.00	0.50	0.50	0.00
27	Gogebic sil, 6 to 18% slopes, very stoney, rocky	10	0.00	0.20	0.80	0.00	0.00
28	Gogebic sil, 6 to 18% slopes, very stoney, rocky	15	0.00	0.27	0.60	0.13	0.00
36	Gogebic-Metonga fsl 2 to 10% Slopes	11	0.00	0.00	0.36	0.55	0.09
37	Gogebic-Metonga fsl 2 to 10% Slopes	14	0.00	0.00	0.36	0.50	0.14
38	Gogebic-Metonga fsl 2 to 10% Slopes	11	0.00	0.00	0.36	0.45	0.19
39	Gogebic-Metonga fsl 2 to 10% Slopes	14	0.00	0.00	0.21	0.71	0.08
40	Gogebic-Metonga fsl 2 to 10% Slopes	12	0.00	0.00	0.42	0.58	0.00
41	Gogebic-Metonga fsl 2 to 10% Slopes	16	0.00	0.00	0.13	0.81	0.06

EMI:

Alternative methods for mapping soils and soil properties are being evaluated by NRCS. The availability of computers, global positioning systems (GPS), geographical information systems (GIS), and geophysical tools are changing the way we look at and map soils. Because of their speed and ease of use, electromagnetic induction (EMI) has significant advantages over conventional soil survey techniques. The efficiency of EMI promotes the collection of larger data sets than is possible with conventional soil survey techniques. Because of the larger number of observations, maps prepared from EMI data can provide higher levels of resolution than soil maps prepared with conventional methods (Jaynes, 1995). In many areas, spatial patterns of apparent conductivity correspond well with the soil patterns shown on soil survey maps. For high intensity soil mapping, maps of apparent conductivity have been recommended as a *surrogate* for soil survey maps (Jaynes, 1995).

EMI uses electromagnetic energy to measure the apparent conductivity of earthen materials. Apparent conductivity is a weighted, average conductivity measurement for a column of earthen materials to a specific depth (Greenhouse and Slaine, 1983). With EMI, a transmitter produces a magnetic field that induces current to flow through the subsurface. This flow of current sets up a secondary magnetic field in the soil. By comparing the difference in the magnitude and phase of these magnetic fields, the device measures the apparent conductivity of the profiled materials. No ground contact is needed with EMI.

Variations in apparent conductivity are produced by changes in the electrical conductivity of earthen materials. The electrical conductivity of soils is influenced by the type and concentration of ions in solution, the amount and type of clays in the soil matrix, the volumetric water content, and the temperature and phase of the soil water (McNeill, 1980). The apparent conductivity of soils will increase with increases in soluble salt, water, and clay contents (Kachanoski et al., 1988; Rhoades et al., 1976).

Interpretations of EMI data are based on the identification of spatial patterns within data sets. Though seldom diagnostic in themselves, lateral and vertical variations in apparent conductivity have been used to infer changes in soils and soil properties. EMI integrate the bulk physical and chemical properties of a soil within a defined depth into a single value. As a consequence, measurements can be associated with changes in soil properties, soils, and soil map units (Hoekstra et al., 1992; Jaynes et al., 1993; Doolittle et al., 1996). For each soil, intrinsic physical and chemical properties, as well as temporal variations in soil water and temperature, result in a unique or characteristic range of apparent conductivity values.

Study Site:

The study site was located in the southwest quarter of Section 31, T. 48 N., R. 5 W., in Bayfield County. The site is located within an idle field. This study site is in an area that has been mapped as Alcona fsl, 4 to 10 % slopes; Portwing-Herbster; and Cublake-Croswell-Ashwabay 5 % slopes.

Table 4. Classification of soils surveyed with EMI.

Soil Series	Taxonomic Classification
Allendale	sandy over clayey, mixed, semiactive, frigid Alfic Epiaquods
Ashwabay	sandy, mixed, frigid Alfic Oxyaquic Haplorthods
Cublake	sandy, mixed, frigid Oxyaquic Haplorthods
Kellogg	sandy over clayey, mixed, active, frigid Alfic Oxyaquic Haplorthods
Herbster	fine, mixed, superactive, frigid Aeric Glossaqualfs
Portwing	fine, mixed, superactive, frigid Oxyaquic Glossudalfs

The taxonomic classifications of the soils surveyed with EMI are shown in Table 4. The very deep, well drained Alcona soil formed in stratified sandy and loamy glaciofluvial and glacialacustrine deposits. Alcona is a member of the coarse-loamy, mixed, active, frigid Alfic Haplorthods family. The very deep, somewhat poorly drained Allendale soil formed in sandy sediments and in the underlying clayey lacustrine or till deposits. The very deep, moderately well drained Ashwabay soil formed in sandy outwash or beach deposits underlain by clayey glacial till

or lacustrine deposits. The very deep, moderately well drained Croswell soil formed in sandy glacial drift. Croswell is a member of the sandy, mixed, frigid Oxyaquic Haplorthods family. The very deep, moderately well drained Cublake soils formed in deep sandy outwash underlain by stratified silty, loamy, and sandy glaciofluvial deposits. The very deep, moderately well drained Kellogg soils that formed in sandy lacustrine or outwash sediments, underlain by clayey lacustrine deposits. The very deep, somewhat poorly drained Herbster soil formed in clayey till and in the underlying loamy and sandy stratified lacustrine deposits. The very deep, moderately well drained Portwing soils formed in clayey till over stratified loamy and sandy lacustrine deposits.

Field Procedures:

Survey procedures were simplified to expedite fieldwork. At each site, two parallel lines were laid out. Along each line, survey flags were inserted in the ground at intervals of about 30 m. These flags served as grid line end points and provided some measure of ground control. The two parallel lines enclosed a rectangular grid area. Dimensions of the grids were 240 by 240 m (about 5.76 ha) at Study Site 1 and 150 by 150 m (about 2.25 ha) at Study Site 2.

Walking at a fairly uniform pace across the field in a back and forth pattern with an EM38DD meter completed the survey. The EM38DD meter was operated in the continuous mode with measurements recorded at a 1-sec interval. The meter was orientated with its long axis parallel to the direction of traverse. The meter was held about 3 inches above the ground surface and operated with the DAS70 data acquisition system.

Results:

Table 3 summarizes the results of this survey. Within this site, apparent conductivity ranged from -2.9 to 21.2 mS/m. Negative values are attributed to calibration errors and surface or near-surface metallic artifacts. With the EM38DD meter, apparent conductivity increased and became slightly more variable with increasing depth. In the shallower-sensing, horizontal dipole orientation (0 to 0.75 m), apparent conductivity averaged about 7.5 mS/m with a standard deviation of about 4 mS/m. In the deeper-sensing, vertical dipole orientation (0 to 1.5 m), apparent conductivity averaged 9.1 mS/m with a standard deviation of about 5.2 mS/m. The increased conductivity with increasing depth was attributed to greater moisture and clay contents at lower soil depths.

Table 3. Basic EMI Statistics for Study Site

	EM38DD-H	EM38DD-V
Observations	1331	1331
Mean	7.5	9.1
Standard Deviation	4	5.2
Minimum	-2.9	-0.04
Maximum	16.7	21.2
25%-tile	4.7	4.6
75%-tile	10.5	13.5

Figure 1 contains plots showing the spatial distribution of apparent conductivity collected with the EM38DD meter. In each plot, colors have been used to show the distribution of apparent conductivity. In each plot the isoline interval is 3 mS/m. To remove spurious measurements and lines, the *grid node editor* of Surfer 8 was used to blank or make slight changes (0.1 to 0.2 mS/m) to some of the measured EMI responses.

Figure 1 reveal that, for data collected with the four EMI instruments, broad spatial patterns of apparent conductivity are reasonably similar in each dipole orientation. A conspicuous ribbon of higher apparent conductivity identifies a lower-lying area along a drainage channel that extends in a north-south direction across the central portion of the survey area. The higher conductivity is explained by higher clay and moisture (somewhat poorly drained) contents. The higher conductivity in the southwestern (lower left-hand) portion of these plots generally conforms to The relatively high conductivity is associated with the higher moisture content of. Other portions of survey area consists of higher-lying plane and convex surfaces that are better drained and mapped as areas of Bosket fine sandy loam, 4 to 10 % slopes.

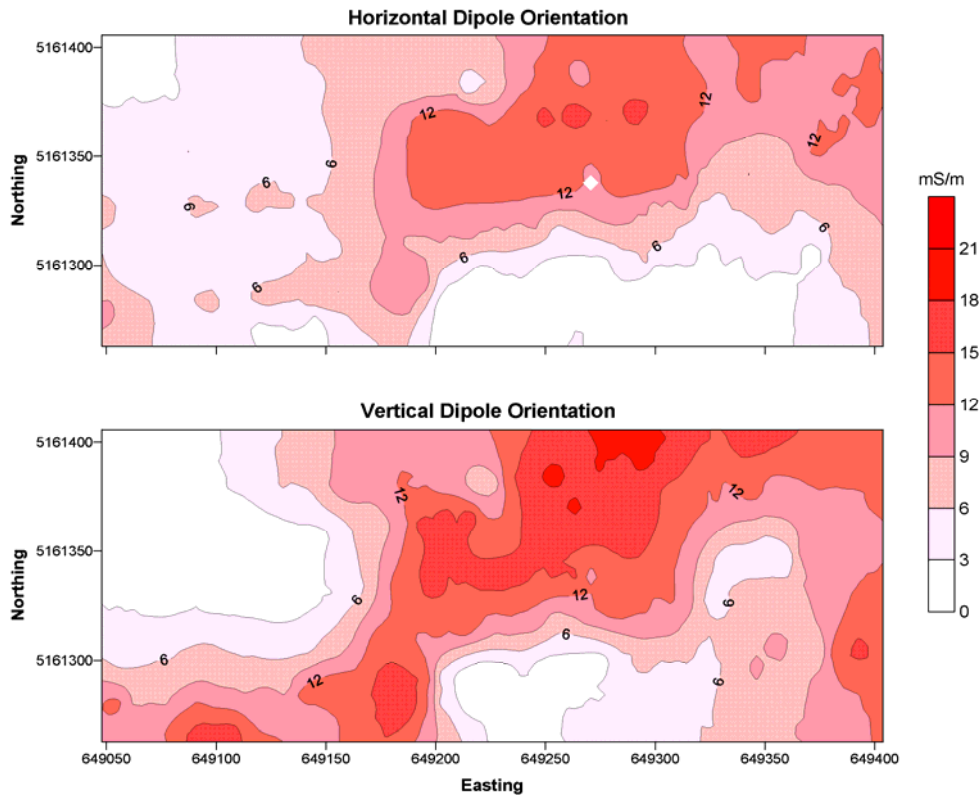


Figure 1. Apparent conductivity data collected with an EM38DD meter in area of Alcona, Portwing, Herbster, Cublake, Crosswell and Ashwabay soils.

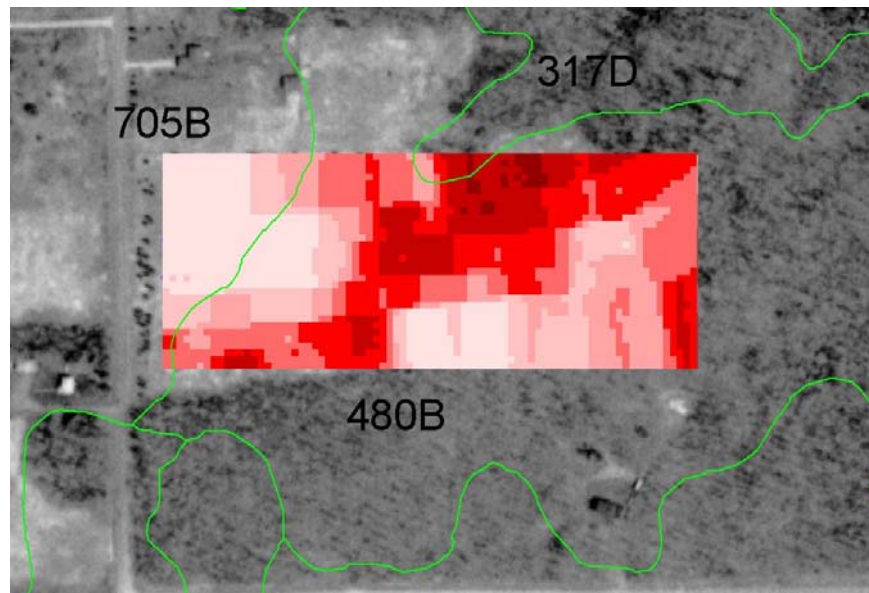


Figure 2. Soil map with the EC_a data from the study site overlain.

References:

- Birkhead, A. L., G. L. Heritage, H. White, and A. W. van Niekerk. 1996. Ground-penetrating radar as a tool for mapping the phreatic surface, bedrock profile, and alluvial stratigraphy in the Sabie River, Kruger National Park. *J. Soil and Water Cons.*, 51(3): 234-241.
- Collins, M. E., J. A. Doolittle, R. V. Rourke. 1989. Mapping depth to bedrock on a glaciated landscape with ground-penetrating radar. *Soil Sci. Soc. Am. J.*, 53(3): 1806-1812.
- Daniels, D. J. 1996. *Surface-Penetrating Radar*. The Institute of Electrical Engineers, London, United Kingdom. 300 p.
- Doolittle, J. A. 1987. Using ground-penetrating radar to increase the quality and efficiency of soil surveys. 11-32 pp. In: Reybold, W. U. and G. W. Peterson (eds.) *Soil Survey Techniques*, Soil Science Society of America. Special Publication No. 20. 98 p.
- Doolittle, J., R. Murphy, G. Parks, and J. Warner. 1996. Electromagnetic induction investigations of a soil delineation in Reno County, Kansas. *Soil Survey Horizons* 37:11-20.
- Geonics Limited. 2000. EM38DD ground conductivity meter: Dual dipole version operating manual. Geonics Ltd., Mississauga, Ontario.
- Geophysical Survey Systems, Inc, 2001a. RADAN for Windows NT; User's Manual - Condensed. Manual MN43-132 Rev C. Geophysical Survey Systems, Inc., North Salem, New Hampshire.
- Greenhouse, J. P., and D. D. Slaine. 1983. The use of reconnaissance electromagnetic methods to map contaminant migration. *Ground Water Monitoring Review* 3(2): 47-59.
- Hoekstra, P., R. Lahti, J. Hild, R. Bates, and D. Phillips. 1992. Case histories of shallow time domain electromagnetics in environmental site assessments. *Ground Water Monitoring Review*. 12(4): 110-117.
- Jaynes, D. B. 1995. Electromagnetic induction as a mapping aid for precision farming. pp. 153-156. IN: *Clean Water, Clean Environment, 21st Century: Team Agriculture. Working to Protect Water Resources*. Kansas City, Missouri. 5 to 8 March 1995.
- Jaynes, D. B., T. S. Colvin, J. Ambuel. 1993. Soil type and crop yield determination from ground conductivity surveys. 1993 International Meeting of American Society of Agricultural Engineers. Paper No. 933552. ASAE, St. Joseph, MI.
- Kachanoski, R. G., E. G. Gregorich, and I. J. Van Wesenbeeck. 1988. Estimating spatial variations of soil water content using noncontacting electromagnetic inductive methods. *Can. J. Soil Sci.* 68:715-722.
- McNeill, J. D. 1980. Electrical Conductivity of soils and rocks. Technical Note TN-5. Geonics Ltd., Mississauga, Ontario. p. 22.
- Morey, R. M. 1974. Continuous subsurface profiling by impulse radar. p. 212-232. IN: *Proceedings, ASCE Engineering Foundation Conference on Subsurface Exploration for Underground Excavations and Heavy Construction*, held at Henniker, New Hampshire. Aug. 11-16, 1974.
- Rhoades, J. D., P. A. Raats, and R. J. Prather. 1976. Effects of liquid-phase electrical conductivity, water content, and surface conductivity on bulk soil electrical conductivity. *Soil Sci. Soc. Am. J.* 40:651-655.
- Won, I. J., Dean A. Keiswetter, George R. A. Fields, and Lynn C. Sutton. 1996. GEM-2: A new multifrequency electromagnetic sensor. *Journal of Environmental & Engineering Geophysics* 1:129-137.